catalysts

MDPI

Article

Structural Properties and Catalytic Activity of Binary Poly (vinyl alcohol)/Al_2O_3 Nanocomposite Film for Synthesis of Thiazoles

Sayed M. Riyadh [1,3], Khaled D. Khalil [2,3,*] and Ali H. Bashal [2]

[1] Department of Chemistry, Faculty of Science, Taibah University, Al-Madinah Almunawrah 30002, Saudi Arabia; riyadh1993@hotmail.com
[2] Department of Chemistry, Faculty of Science, Taibah University, Al-Madinah Almunawrah, Yanbu 46423, Saudi Arabia; abishil@taibahu.edu.sa
[3] Department of Chemistry, Faculty of Science, Cairo University, Giza 12613, Egypt
* Correspondence: khd.khalil@yahoo.com

Received: 14 December 2019; Accepted: 7 January 2020; Published: 10 January 2020

Abstract: A solution casting technique was applied to prepare a binary poly (vinyl alcohol)/Al_2O_3 nanocomposite. The structural properties of nanocomposite were investigated using Fourier-transform infrared spectra, field emission scanning electron microscope, energy dispersive X-ray analyses, and X-ray diffraction. The hybrid PVA/Al_2O_3 film exhibited a conspicuous catalytic performance for synthesis of thiazole derivatives under mild reaction conditions. Moreover, the optimization of catalytic efficiency and reusability of this nanocomposite have been investigated.

Keywords: poly (vinyl alcohol); aluminum oxide; nanocomposite; heterogeneous catalysis; thiazoles

1. Introduction

Polyvinyl alcohol (PVA) is a biodegradable, water-soluble, and environmentally benign polymeric material with unique emulsifying, adhesive, and film-forming properties [1]. It can be used in the synthesis of organic-inorganic hybrid membrane for biodiesel production [2] and has been regarded as appropriate matrix in microbial fuel cell applications [3]. PVA has also been used in production of biomedical hydrogels with high ability to swell [4]. Moreover, diversity of industrial applications of PVA has been reported such as optical and humidity sensors, food packaging, surgical devices, manufacture of polarizing sheet, and production of thin film transistors [5,6]. Recently, many industrial applications of aluminum oxide (Al_2O_3) nanoparticles have been disseminated such as; drilling fluids agent [7], separators for lithium batteries [8], and biosensors for vitamin E [9]. Aluminum oxide nanoparticles were also used to enhance the thermal and mechanical properties of wood fibers [10]. Conspicuously, aluminum oxide nanoparticles, with large surface area and pore-size distribution, have superior catalytic activities for diverse organic reactions [11,12]. Recently, metal oxide nanoparticles embedded within the polymer matrix have attracted growing interest due to the unique properties that displayed by the hybrid nanocomposites. The properties of the created nanocomposites depend on many factors like the method of preparation, the morphological structure of the prepared nanocomposite, nature of metal oxide nanoparticles that incorporated in, the structural features of the polymer used, and the chemical properties of both metal oxide and polymer molecules. The physicochemical properties of the nanosized particles within the hybrid material differ markedly from those of molecular and bulk materials. In our previous work we have concluded that, the synergistic interaction between polymers and inorganic nanoparticles leads to simulative formation of polymer/inorganic nanocomposite with novel catalytic performance for synthesis of different azoles [13,14]. The preparation of PVA/Al_2O_3 composites has received much attention in the past few years for various applications [15,16]. The purpose of this study is the preparation of new PVA/Al_2O_3 thin film nanocomposite by using simple solution casting method (Figure 1). Moreover, the nanocomposite hybrid material was characterized and investigated as powerful recyclable catalyst for synthesis of bioactive azoles.

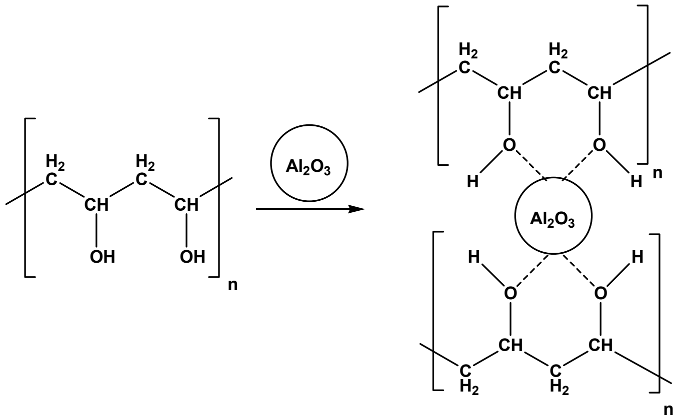

Figure 1. Structure of a PVA-Al_2O_3 nanocomposite.

2. Results and Discussion.

2.1. Characterization of PVA/Al_2O_3 Composite Film

2.1.1. Fourier-Transform Infrared (FTIR) Spectra

The FTIR spectra of virgin PVA [17] and PVA-Al_2O_3 film were measured and the assignment of the most evident absorption bands are shown in Figure 2. The FTIR spectra of virgin PVA revealed an intense and broad stretching band at υ = 3319 cm^{-1} and another bending vibration at υ = 1634 cm^{-1} assignable to hydroxyl group. In addition, there is a clear decrease in the intensity of these bands for the hybrid PVA-Al_2O_3 film, which is attributed to the interaction with Al ions [18] and the influence of the drying temperature. Also, the absorption bands at υ = 2945 and 1428 cm^{-1} appeared as a result of stretching and bending vibrations of (CH) and (CH_2) groups respectively. The broad absorption peak at υ = 1091 cm^{-1} indicates the C–O stretching vibration [19]. In the finger print region for the spectra of hybrid PVA-Al_2O_3 film, two characteristic peaks at υ = 627 and 579 cm^{-1} of Al_2O_3 [12] are shown as an evidence for the incorporation of Al_2O_3 molecules in the polymer matrix. Finally, the shift and the intensity decrease in all bands were familiar as result of the interaction between the PVA and metal oxide.

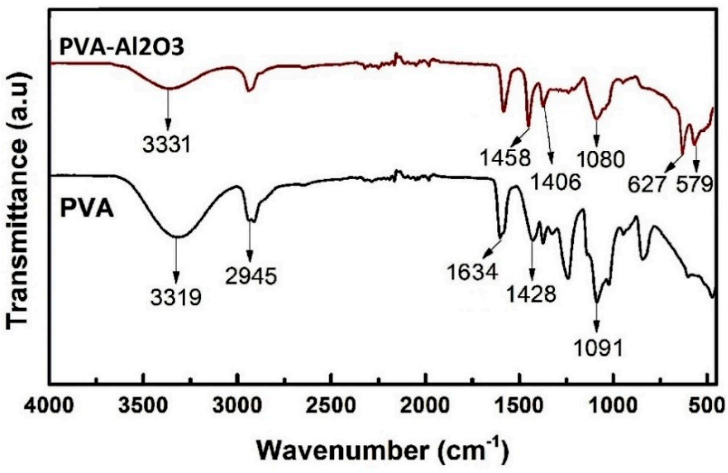

Figure 2. FTIR of original PVA and PVA-Al_2O_3 (10 wt%) nanocomposite.

2.1.2. Field Emission Scanning Electron Microscope (FESEM) and Energy Dispersive X-ray (EDX) Analyses

FESEM was applied to study the morphological changes in PVA with the incorporation of Al_2O_3 molecules. FESEM micrographs of the virgin PVA, Al_2O_3 nanoparticles, and the hybrid PVA-Al_2O_3 composite are shown in Figure 3. The surface of the unmodified PVA (Figure 3a) was obtained to be smooth and homogeneous with great extent as compared to the hybrid composite film (Figure 3c). As shown in the micrographs, the surface of polymer was highly deformed upon metal oxide interaction and the metal oxide particles appeared as bright spots that were homogeneously distributed throughout the polymer surface, which has a great similarity to the morphological surface of Al_2O_3 nanoparticles as shown in Figure 3b. Moreover, energy dispersive X-ray (EDX) measurements for the modified PVA-Al_2O_3 composite film confirmed the presence of alumina inside the PVA matrix. From the EDX results, the elemental analysis of modified composite determined the Al_2O_3 content in the matrix to be 10 wt% (Figure 4).

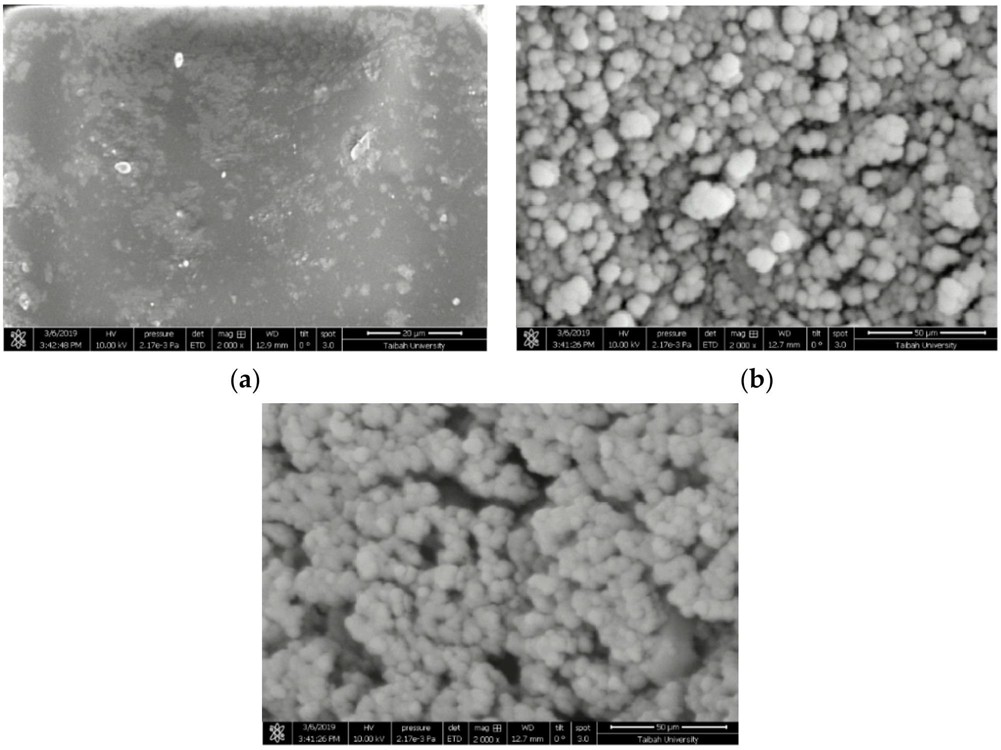

(**a**) (**b**)

(**c**)

Figure 3. (**a**) SEM image of PVA; (**b**) SEM image of Al_2O_3 nanoparticles; and (**c**) SEM image of PVA/A_2O_3 film.

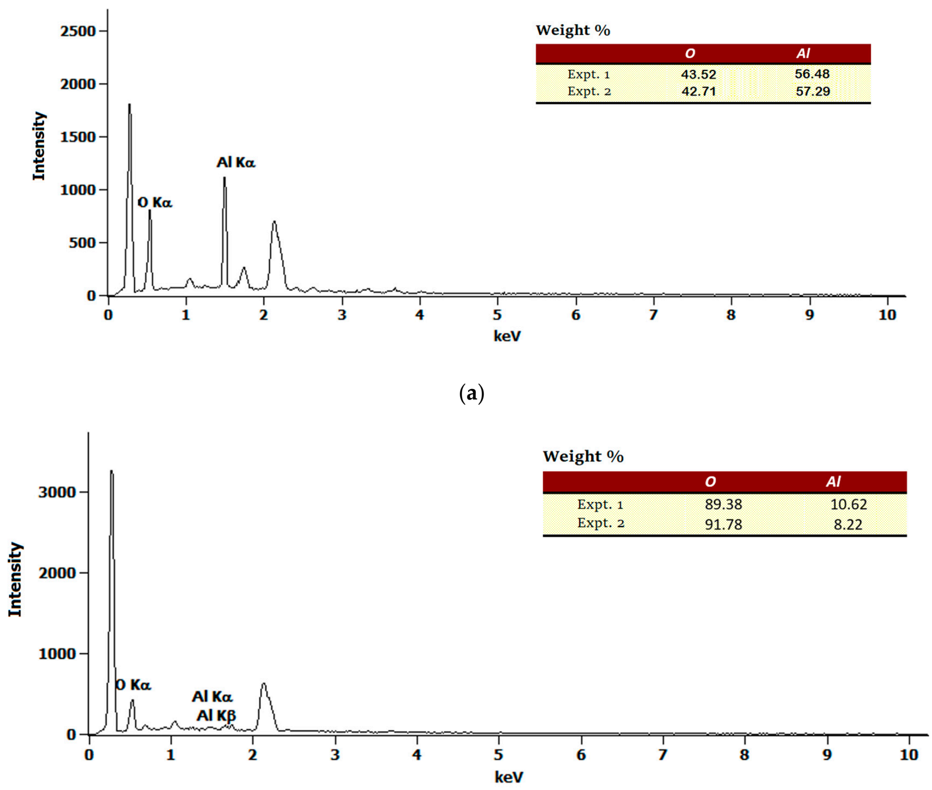

(**a**)

(**b**)

Figure 4. (**a**) energy dispersive X-ray (EDX) spectra of Al_2O_3 nanoparticles and (**b**) EDX spectra of PVA-Al_2O_3 (10 wt%).

2.1.3. Structure Analysis

X-ray diffraction (XRD) patterns of the control PVA (obtained under the same conditions but in absence of alumina powder) and the PVA-Al_2O_3 thin film composite were shown in Figure 5. The pattern of control PVA contains only a characteristic sharp peak at $2\ \theta = 20°$ as reported in literature [20]. For the PVA-Al_2O_3 composite pattern there was a clear broad hump that indicates the majority of the amorphous nature of virgin PVA. It is obviously seen that the relatively higher sharpness of the diffraction peaks a bit with the incorporation of Al_2O_3 particles, which indicates the interaction with alumina results in a clear decrease in the PVA crystallinity. Moreover, the disappearance of the characteristic Al_2O_3 peaks (ASTM 75-1862) and the lower crystallinity of the PVA-Al_2O_3 nanocomposite are attributed to the strong interaction between Al_2O_3 and PVA [16].

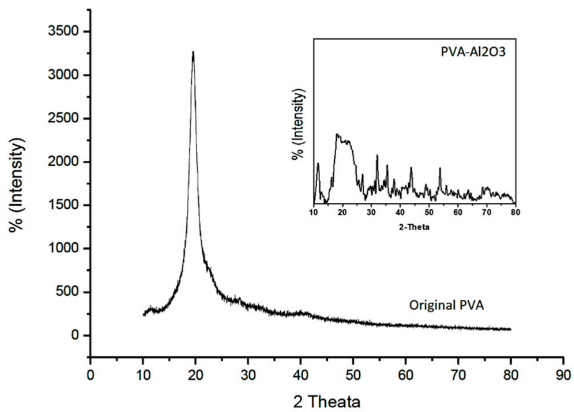

Figure 5. XRD pattern of virgin PVA and PVA-Al_2O_3 nanocomposite.

2.2. Synthesis of Thiazole Derivatives

The reaction conditions between thiosemicarbazones and α-haloketones or α-haloesters were optimized based on the model reaction of 2-benzylidenehydrazine-1-carbothioamide (**1a**) and ethyl 2-chloro-3-oxobutanoate (**2a**) to estimate the proper catalytic loading and time (Scheme 1 and Table 1).

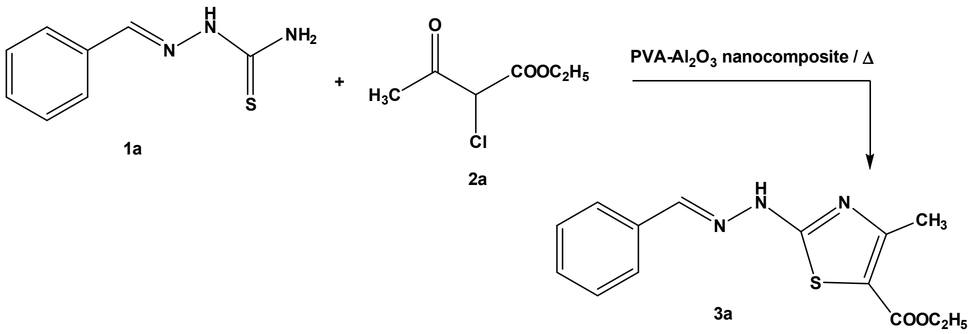

Scheme 1. Synthesis of **3a** as a model product.

Table 1. Optimization of catalytic loading of PVA-Al_2O_3 nanocomposite as a basic catalyst.

Entry	Loading Catalyst (Wt%; *)	Time (min)	Yield (%)	Entry	Loading Catalyst (Wt%; *)	Time (min)	Yield (%)
1	2.5	60	40	7	10	30	40
2	5	60	50	8	10	60	60
3	10	60	60	9	10	90	72
4	15	60	60	10	10	120	80
5	20	60	59	11	10	150	87
6	25	60	56	12	10	180	92

(*) Method A, by using 10 wt% of PVA/Al_2O_3 nanocomposite film as basic catalyst.

As shown in Table 1, the reactions were proceeded in dioxane under thermal conditions with a loading weight percentage of (2.5%, 5%, 10%, 15%, 20%, and 25%) PVA-Al_2O_3 nanocomposite as a basic catalyst. The results indicated that, the optimal loading catalyst was 10 wt% (entry 3) for the reaction time 60 min. In addition, the reactions were screened to estimate the optimal time. It was noted that, the formation of thiazole product **3a** was significantly increased with time (entries 7–12). Thus, the maximum yield percent was obtained after 180 min (entry 12), which produced the product **3a** with 92% yield. Moreover, the recyclability of PVA-Al_2O_3 nanocomposite as a basic catalyst was also investigated. The catalyst was reused three times without significant loss of its catalytic efficiency (Table 2) under optimum conditions (10 wt% and 180 min).

Table 2. Recyclability of PVA-Al_2O_3 nanocomposites as basic catalyst.

State of Catalyst	Fresh Catalyst	Recycled (1)	Recycled (2)	Recycled (3)
Yield (%) of product 3a (*)	92	91	90	90

(*) Method A, by using 10 wt% of PVA/Al_2O_3 nanocomposite film as basic catalyst.

Subsequently, a wide array of 2-arylidenehydrazine-1-carbothioamides (**1a–g**), bearing electron-donating or electron-withdrawing group, and α-haloesters **2a** or α-haloketones **2b** were refluxed in dioxane for 3h, under different conditions, and provided 2-hydrazinothiazoles **3a–j** (Scheme 2 and Table 3).

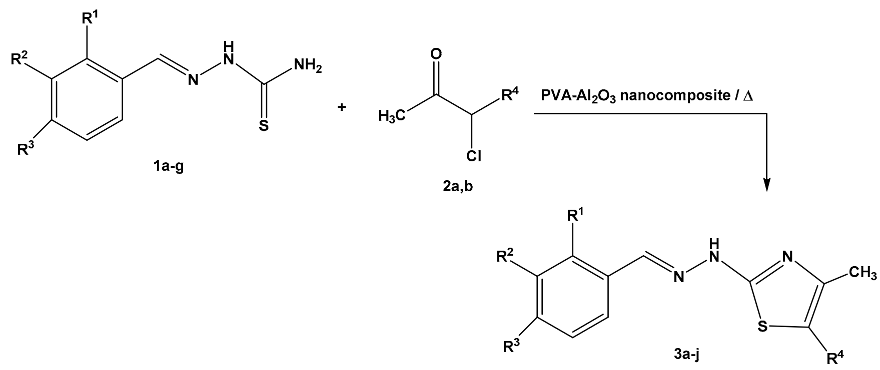

Scheme 2. Synthesis of thiazole derivatives **3a**–**j**.

Table 3. Yield percent of products **3a**–**j.**

Compd. No.	R^1	R^2	R^3	R^4	Yield (%)			M.P. (°C)	Ref.
					No Catalyst	Al_2O_3 (*)	PVA/Al_2O_3 (**)		
3a	H	H	H	COOEt	78	90	92	195–197	[21]
3b	H	H	Cl	COOEt	77	87	90	205–207	[21]
3c	H	H	NO_2	COOEt	-	-	94	260–262	[21]
3d	H	H	$N(CH_3)_2$	COOEt	-	-	95	230–232	[21]
3e	H	H	OCH_3	COOEt	-	-	95	180–182	[21]
3f	Cl	H	Cl	COOEt	-	-	92	222–224	[21]
3g	H	OCH_3	OH	COOEt	-	-	97	226–228	[21]
3h	H	H	H	$COCH_3$	-	-	93	222–224	[22]
3i	H	H	OCH_3	$COCH_3$	-	-	91	214–216	[22]
3j	Cl	H	Cl	$COCH_3$	-	-	96	240–242	[22]

(*) Method B in experimental part. (**) Method A in experiment part.

As shown in Table 3, the comparative study for the yield percentage of the products **3a** and **3b** under different reaction conditions, namely blank experiments (without catalyst), control experiments (Al_2O_3 nanoparticles), and PVA/Al_2O_3 nanocomposite film was investigated. The yield was enhanced in the presence of the later basic catalysts. Although the catalytic performance of both basic catalysts were quite similar, PVA/Al_2O_3 nanocomposite film was more superior due to the ease of its recyclability and also a relatively smaller amount of Al_2O_3 was required in the catalyst preparation.

A plausible mechanism for synthesis of 2-hydrazinothiazoles **3a–j** using PVA/Al_2O_3 nanoparticles was depicted in Scheme 3.

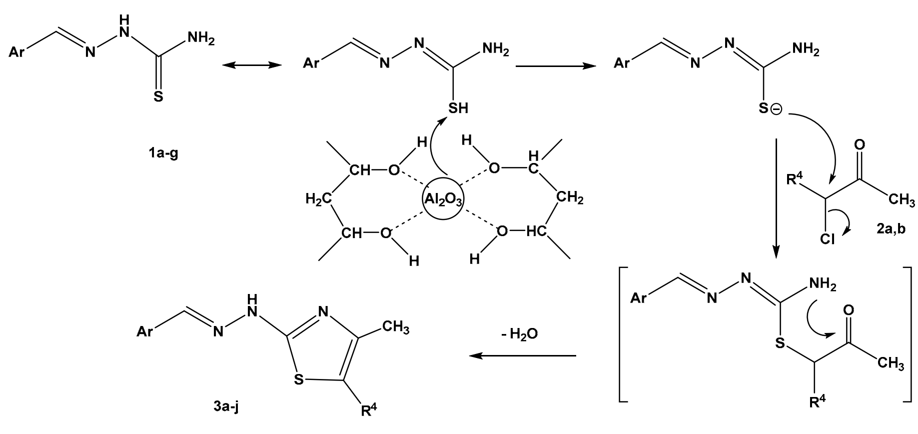

Scheme 3. Plausible mechanism for synthesis of 2-hydrazinothiazoles **3a**–**j**.

Al_2O_3 nanoparticles act as a Bronsted base [11] via deprotonation of the thiol group of 2-arylidenehydrazine-1-carbothioamide (**1a–g**). The producing thiolate anion attacks α−halocarbonyl compounds (2a,b) with displacement of chlorine atom to give non-isolable intermediate. Cyclocondensation of the latter intermediate afforded the authenticated thiazole derivatives **3a–j**.

3. Materials and Methods

PVA (molecular weight = 22,000 g/mol, density = 1.19 g/cm^3), Al_2O_3 nanoparticles (Merck 642991; 30–60 nm particle size (TEM); 20 wt% in water), and ethylenediamine (ED) were purchased by Sigma Aldrich. Thiosemicarbazones **1a–g** were prepared as reported in literature [23–27]. Melting points of authenticated samples **3a–j** were measured on an electrothermal Gallenkamp capillary apparatus (Leicester, UK). The FTIR spectra of nanocomposite were recorded on a Pye-Unicam SP300 Instrument (Cambridge, UK) in potassium bromide discs. FESEM analyses were measured on a high resolution scanning electron microscope (model HRSEM, JSM 6510A, Jeol, Tokyo, Japan). XRD measurement was carried out on Philips Diffractometer (Model: X'Pert-Pro MPD; Philips, Eindhoven, The Netherland).

3.1. Preparation of PVA-Al_2O_3 Composite Films

The PVA and Al_2O_3 hybrid composite was prepared using the simple solution casting method. Initially, 0.5 g of PVA was dissolved in deionized water (50 mL) under stirring for 6 h at 80 °C then, 0.1 g of Al_2O_3 nanoparticles was added to the latter PVA solution and the mixture was kept under magnetic stirring for 1 h till a dispersion viscous solution was formed. The produced viscous solution was casted in a pre-cleaned Teflon Petri-dish and this solution was annealed in an oven adjusted at 150 °C for 1 h. The final PVA-Al_2O_3 films for the study was 125 mm × 12 mm × 1.5 mm in dimensions. Furthermore, a pure PVA film, without Al_2O_3, was prepared in a similar way for comparative studies (Figure 6).

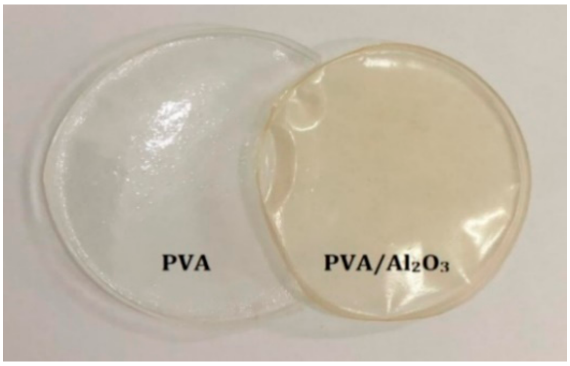

Figure 6. Images of virgin PVA and PVA-Al_2O_3 nanocomposite.

3.2. General Procedures for the Synthesis of 2- Hydrazonothiazoles **3a-j**

Method A: A mixture of thiosemicarbazones **1a–g** (1 mmol) in dry dioxane (20 mL), containing PVA/Al_2O_3 film (0.1 g, 10% wt relative to thiosemicarbazones), and ethyl 3-chloro-2-oxobutanoate (**2a**) or 3-chloro-2,4-pentanedione (**2b**) (1 mmol of each) was refluxed until all the starting material was consumed (3 h. as monitored by TLC). After completion of the reaction, the hot solution was filtered to remove the film and the filtrate was poured into 50 mL ice/50 mL, 6 M HCl mixture. The precipitate was filtered, washed with water, and crystallized from appropriate solvent to give authenticated thiazole derivatives **3a–j** [21,22]. The film was washed with hot ethanol and dried in an oven adjusted at 150 °C for 1 h to be reused following the same procedure in method A.

Method B: the same procedure in method A was applied using Al_2O_3 nanoparticles instead of PVA-Al_2O_3 film. After the completion of the reaction, the solution was poured into 50 mL ice/50 mL, 6 M HCl mixture to get rid of Al_2O_3 nanoparticles.

4. Conclusions

In this work, a new hybrid PVA/Al_2O_3 nanocomposite was prepared via simple solution casting method and the obtained hybrid nanocomposite film exhibited an obvious catalytic performance for synthesis of 2-hydrazonothiazoles with an excellent yield. The optimal loading catalyst was 10 wt% and the catalyst was reused effectively three times without significant loss of its catalytic efficiency.

Author Contributions: Both S.M.R. and K.D.K. suggested the plan of the article. K.D.K. interpreted the results of preparation of catalyst, and S.M.R. interpreted the chemistry part. A.H.B. participated in the reviewing and publication processes of the article. All authors have read and agreed to the published version of the manuscript.

Funding: This research received no external funding.

Conflicts of Interest: The authors declare no conflict of interest.

References

1. Puga, A.V.; Garcia-Valls, R.; Fernández-Prieto, S.; Smets, J.; York, D. Dual xanthan gum/poly (vinyl acetate) or alkyl-functionalized poly (vinyl alcohol) films as models for advanced coatings. *J. Appl. Polym. Sci.* **2014**, *131*, 40870–40880. [CrossRef]
2. Li, M.; Zhang, W.; Zhou, S.; Zhao, Y. Preparation of poly (vinyl alcohol)/palygorskite-poly (ionic liquids) hybrid. *Sep. Purif. Technol.* **2020**, *230*, 115746. [CrossRef]
3. Chakraborty, I.; Das, S.; Dubey, B.K.; Ghangrekar, M.M. Novel low cost proton exchange membrane made from sulphonated biochar for application in microbial fuel cells. *Mater. Chem. Phys.* **2020**, *239*, 122025. [CrossRef]
4. Mandru, M.; Bercea, M.; Gradinaru, L.M.; Ciobanu, C.; Drobota, M.; Vlad, S.; Albulescu, R. Polyurethane/poly (vinyl alcohol) hydrogels: Preparation, characterization and drug delivery. *Eur. Polym. J.* **2019**, *118*, 137–145. [CrossRef]
5. Zhang, B.; Zhou, M.; Liu, X. Monolayer assembly of oriented zeolite crystals on α-Al_2O_3 supported polymer thin films. *Adv. Mater.* **2008**, *20*, 2183–2189. [CrossRef]
6. Prajapati, G.K.; Gupta, P.N. Comparative study of the electrical and dielectric properties of PVA-PEG-Al_2O_3-MI (M = Na, K, Ag) complex polymer electrolytes. *Phys. B Condens. Matt.* **2011**, *406*, 3108–3113. [CrossRef]
7. Smith, S.R.; Rafati, R.; Haddad, A.S.; Cooper, A.; Hamidi, H. Application of aluminum oxide nanoparticles to enhance rheological and filtration properties of water based muds at HPHT conditions. *Coll. Surf. A* **2018**, *537*, 361–371. [CrossRef]
8. Wei, N.; Hu, J.; Zhang, M.; He, J.; Ni, P. Cross-linked porous polymer separator using vinyl-modified aluminum oxide nanoparticles as cross-linker for lithium-ion batteries. *Electrochim. Acta* **2019**, *307*, 495–502. [CrossRef]
9. Parvin, M.H.; Arjomandi, J.; Lee, J.Y. γ-Al_2O_3 nanoparticle catalyst mediated polyaniline gold electrode biosensor for vitamin E. *Catal. Commun.* **2018**, *110*, 59–63. [CrossRef]
10. Gupta, A.; Kumar, A.; Sharma, K.V.; Gupta, R. Application of High Conductive Nanoparticles to Enhance the Thermal and Mechanical Properties of Wood Composite. *Mater. Today Proc.* **2018**, *5*, 3143–3149. [CrossRef]
11. Zarnegar, Z.; Shokrani, Z.; Safari, J. Asparagine functionalized Al_2O_3 nanoparticle as a superior heterogeneous organocatalyst in the synthesis of 2-aminothiazoles. *J. Mol. Struct.* **2019**, *1185*, 143–152. [CrossRef]
12. Goudarzi, M.; Ghanbari, D.; Salavati-Niasari, M.; Ahmadi, A. Synthesis and Characterization of $Al(OH)_3$, Al_2O_3 Nanoparticles and Polymeric Nanocomposites. *J. Clust. Sci.* **2016**, *27*, 25–38. [CrossRef]
13. Riyadh, S.M.; Khalil, K.D.; Aljuhani, A. Chitosan-MgO Nanocomposite: One Pot Preparation and Its Utility as an Ecofriendly Biocatalyst in the Synthesis of Thiazoles and [1,3,4] thiadiazoles. *Nanomaterials* **2018**, *8*, 928. [CrossRef]
14. Khalil, K.D.; Riyadh, S.M.; Gomha, S.M.; Ali, I. Synthesis, characterization and application of copper oxide chitosan nanocomposite for green regioselective synthesis of [1,2,3] triazoles. *Int. J. Biol. Macromol.* **2019**, *130*, 928–937. [CrossRef]
15. Mishra, R.; Rao, K.J. Thermal and morphological studies of binary and ternary composites of poly (vinylalcohol) with alumina and zirconia. *Ceram. Int.* **2000**, *26*, 371–378. [CrossRef]

16. Sonmez, M.; Ficai, D.; Stan, A.; Bleotu, C.; Matei, L.; Ficai, A.; Andronescu, E. Synthesis and characterization of hybrid PVA/Al_2O_3 thin film. *Mater. Lett.* **2012**, *74*, 132–136. [CrossRef]
17. Chandar, S.B.; Sathish, S.; Sathyamoorthy, R. Morphology, structure and conduction properties of PVA nano-scale films for field effect organic thin film transistor applications. *Int. J. Nanotechnol. Appl.* **2011**, *5*, 297–308.
18. Qi, Y.N.; Xu, F.; Ma, H.J.; Sun, L.X.; Zhang, J.; Jiang, T. Thermal stability and glass transition behaviour of PANI/γ-Al_2O_3 composites. *J. Therm. Anal. Calorim.* **2008**, *91*, 219–223. [CrossRef]
19. Sugumaran, S.; Bellan, C.S.; Nadimuthu, M. Characterization of composite PVA-Al2O3 thin films prepared by dip coating method. *Iran. Polym. J.* **2015**, *24*, 63–74. [CrossRef]
20. Shakshooki, S.K.; Elejmi, A.A.; Hamassi, A.M.; El-Akari, F.A.; Masoud, N.A. Facile Synthesis of Poly (vinylalcohol)/Fibrous Cerium Phosphate Nanocomposite Membranes. *Sci. Educ.* **2014**, *2*, 1–6.
21. Makam, P.; Kankanala, R.; Parkash, A.; Kannan, T. 2-(2-Hydrazinyl) thiazole derivatives: Design, synthesis and in vitro antimycobacterial studies. *Eur. J. Med. Chem.* **2013**, *69*, 564–576. [CrossRef]
22. Grozav, A.; Gaina, L.I.; Pileczki, V.; Crisan, O.; Silaghi-Dumitrescu, L.; Therrien, B.; Zaharia, V.; Berindan-Neagoe, I. The Synthesis and Antiproliferative Activities of New Arylidene-Hydrazinyl-Thiazole Derivatives. *Int. J. Mol. Sci.* **2014**, *15*, 22059–22072. [CrossRef]
23. Raghav, N.; Kaur, R. Synthesis and evaluation of some semicarbazone- and thiosemicarbazone-based cathepsin B inhibitors. *Med. Chem. Res.* **2014**, *23*, 4669–4679. [CrossRef]
24. Bharti, S.K.; Singh, S.K. Design, synthesis and biological evaluation of some novel benzylidene-2-(4-phenylthiazol-2-yl) hydrazines as potential anti-inflammatory agents. *Med. Chem. Res.* **2014**, *23*, 1004–1015. [CrossRef]
25. Alam, M.S.; Liu, L.; Lee, D.-U. Cytotoxicity of New 5-Phenyl-4,5-dihydro-1,3,4-thiadiazole Analogues. *Chem. Pharm. Bull.* **2011**, *59*, 1413–1416. [CrossRef]
26. Alam, M.S.; Ahmed, J.U.; Lee, D.-U. Synthesis, Antibacterial, Antioxidant Activity and QSAR Studies of Novel 2-Arylidenehydrazinyl-4-arylthiazole Analogues. *Chem. Pharm. Bull.* **2014**, *62*, 1259–1268. [CrossRef]
27. Gingras, B.A.; Hornal, R.W.; Bayley, C.H. The Preparation of Some Thiosemicarbazones and their Copper Complexes. *Can. J. Chem.* **1960**, *38*, 712–719. [CrossRef]